Proceedings of ISFOG 2025
5TH INTERNATIONAL SYMPOSIUM ON
FRONTIERS IN OFFSHORE GEOTECHNICS
Nantes, France | June 9-13 2025

ISBN 978-2-85782-758-0

Numerical study of vibro-driven pile installation in sand

B. Bienen*, P. Kazemi Esfeh, M.F. Bransby
Centre for Offshore Foundation Systems, University of Western Australia, Australia

P. Staubach
Bauhaus-Universität Weimar, Weimar, Germany

**britta.bienen@uwa.edu.au (corresponding author)*

ABSTRACT: Vibro-driving of monopiles is increasingly being considered as it offers advantages of lower acoustic emissions compared to impact-driven piles, rapid installation particularly in sand but also mitigation of the risk of pile run as the pile and vibro-driver remain connected to the crane at all times. Numerical modelling offers the opportunity of providing additional insights that are difficult to obtain through physical modelling, including observation of changes in soil state. Vibro-driving of large diameter thin-walled open-ended cylindrical piles into saturated sand is, in numerical modelling terms, a boundary value problem involving very large deformations (with target penetrations hundreds of times the pile wall thickness), requiring coupled pore fluid-stress analysis with an effective stress-based soil constitutive model that captures the stress and state dependent behaviour of sand. Coupled Eulerian-Lagrangian analysis (together with user-defined routines) has been used here to perform these analyses. Using this approach, this paper explores the complex inter-relation of parameters that can be controlled in vibro-driving and the resulting changes in the pile penetration, which are underpinned by cyclic, dynamic and drainage effects.

Keywords: Monopile; vibro-driving; pile installation; sand; numerical modelling

1 INTRODUCTION

Vibro-driving is increasingly being considered as an installation method for monopiles, due to lower acoustic emissions (and with a different acoustic signature) compared to the percussive impact-driving and rapid yet controlled pile penetration particularly in sand. The pile is held by the vibro-driver through a series of clamps, and the vibro-driver in turn remains connected to the crane at all times. This mitigates the risk of pile run.

Vibro-driving is a dynamic installation method during which vertical vibration cycles are applied to the pile through pairs of counter-rotating eccentric masses in the vibro-driver. These vibrations are de-coupled from the crane via the suppressor housing that forms the upper part of a vibro-driver. The vertical dynamic oscillating force F_{dyn} is proportional to the eccentric moment M_e (in kg.m) and the square of the angular rotation velocity ω where ω is linked to the frequency f:

$$F_{dyn} = M_e \omega^2 \sin \omega t \qquad (1)$$

$$\omega = 2\pi f \qquad (2)$$

The displacement amplitude of the vibro-driver (in air) s_0 relates to

$$s_0 = \frac{M_e}{m_{dyn}} \qquad (3)$$

where m_{dyn} is the dynamic mass. During pile installation, the vibro-driver needs to vibrate the mass of the pile as well as the vibro-driver, which increases m_{dyn} and hence reduces the displacement amplitude. The soil resistance further influences the actual displacement amplitude during pile driving.

The static driving force resulting from the self-weight of the system can be written as

$$F_0 = (m_{dyn} + m_{sup})g - F_{hook} \qquad (4)$$

where m_{sup} is the mass of the suppressor housing, and g is Earth's gravity. The crane may hold back some of the self-weight by applying crane tension or hook load F_{hook}, where pile penetration is expected to be rapid. During easy vibro-driving, pile penetration speed therefore tends to be limited by the crane release speed. The hook load changes the applied static force, but not the mass or the dynamic force and frequency.

Key factors that have been identified as important in vibro-driving include there being sufficient pile upward displacement in the vibration cycles, which (1) leads to full stress reversal on the pile shaft and hence reduces resistance through friction fatigue (e.g. Vogelsang, 2017; Moriyasu et al., 2018; Stein, 2023) and (2) not only unloads the pile tip but also softens the response when resistance is re-mobilised in the following cycle (e.g. Rodger and Littlejohn, 1980; Dierssen, 1994; Massarsch et al., 2020). Dynamic effects may reduce the resistance if the inertial component results in a phase shift that counteracts, in particular, tip resistance mobilisation (Kazemi Esfeh et al., 2025). Excess pore pressures have the potential to further reduce effective stresses and hence facilitate vibro-driven pile installation (e.g. Staubach et al., 2020; Stein, 2023).

The link between vibro-driving 'inputs' (static and vibrating mass, dynamic force, frequency, crane tension) and the resulting response of the pile (in terms of movement amplitudes, soil accelerations and excess pore pressure generation), is indirect, non-unique and complex. The parameters that can be influenced (to some extent) are the frequency, eccentric moment and hence the applied dynamic force, the pile and system dynamic mass and the applied static force (which may differ from the self-weight by the hook load).

This paper discusses results from large deformation coupled pore fluid-stress analyses of a large diameter thin-walled pile being vibro-driven into saturated dense sand. For the same pile geometry and initial soil condition, a pile is vibrated into the seabed using different vibro-driving inputs to explore links between these inputs and the installation progress and resulting changes in soil state around the pile.

2 NUMERICAL MODEL

The numerical model is the same as in Bienen et al. (2021), where the effect of impact-driving on the soil state was investigated, with its flow-on effects to subsequent lateral loading response. The analyses were performed in Abaqus (version 2023) using the Coupled Eulerian-Lagrangian (CEL) approach. In contrast to the analyses discussed in Bienen et al. (2021), which were fully drained, the user routine employed here enables hydro-mechanically coupled analyses to be performed. The approach outlined in Hamann et al. (2015) and Staubach et al. (2020) was adopted. The analyses were performed on the Pawsey Setonix supercomputing facilities (Pawsey, 2023).

2.1 CEL model

The pile was modelled as a rigid body and has a diameter D = 8 m and a wall thickness t such that D/t = 100. An interface roughness of $2/3\tan\varphi_c$ was assigned and the pile was only permitted to displace in the vertical direction. The dynamic mass of the system (pile and vibro-driver) was 1,500 t. The full force due to self-weight was assumed to be 15 MN.

The numerical model is shown in side view in Figure 1, including a void space above the sand to accommodate any soil heave. Taking advantage of symmetry, 90° are modelled.

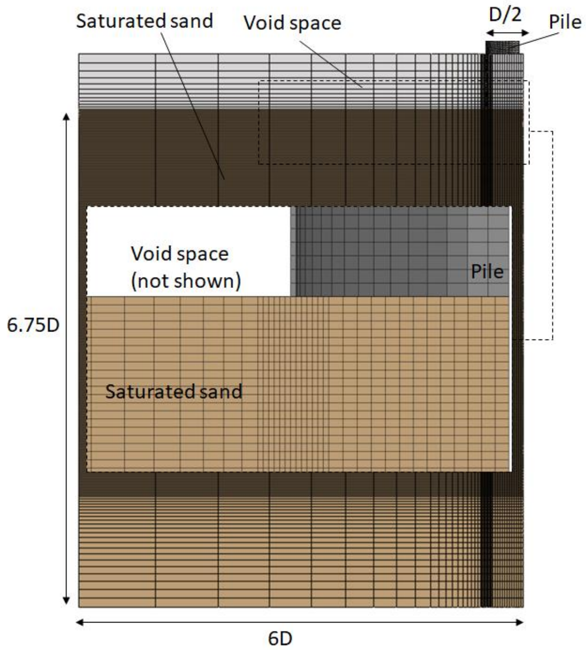

Figure 1. Numerical model

2.2 Soil model and parameters

Karlsruhe fine sand (KFS), a well-researched uniformly graded, fine silica sand, has been selected for the analyses discussed in this paper.

Table 1. Parameters of the hypoplastic model for KFS (Wichtmann and Triantafyllidis, 2016).

Parameter	Value and unit
φ_c	33.1°
h_s	4000 MPa
n	0.27
e_{do}	0.677
e_{co}	1.054
e_{io}	1.212
α	0.14
β	2.5
m_R	2.2
m_T	1.1
R	0.0001
β_R	0.1
χ	5.5

The sand was assumed to be at an initial relative density D_r = 75% and was modelled using the hypoplastic constitutive relation (von Wolffersdorff, 1996; Herle and Niemunis, 1997), with parameters summarised in Table 1. This constitutive model was also used e.g. in Staubach et al. (2020), Bienen et al. (2021; also assuming KFS with D_r = 75%) and Fan et al. (2021) to simulate impact-driven pile installation into (fully drained) sand. As in Staubach et al. (2022), the sand is assumed to be saturated with a permeability $k = 1 \cdot 10^{-4}$ m/s. The bulk modulus of water is taken as 10 MPa for computational efficiency. Drainage is permitted at the soil surface only.

2.3 Overview of analyses

The results of four analyses are discussed in this paper (Table 2), which differ in their vibro frequency and applied dynamic load, with one simulation modelling variation of the hook load.

Table 2. Overview of vibro-driven pile installation analyses.

Name	f (Hz)	F_0 (MN)	F_{dyn} (MN)
V23Hz $F_{dyn}/F_o = 2$	23	15	30
V23Hz $F_{dyn}/F_o = 4$	23	15	60
V15Hz	15	15	25.5
V23Hz hook load	23	3-15	30

Following geostatic equilibrium, corresponding to effective stresses from the effective unit weight of the sand at an initial void ratio $e_0 = 0.771$, the static force corresponding to the self-weight of the pile and vibro-driver, F_0 = 15 MN, was applied linearly increasing followed by a rest time of 2 s. Vibro-driving was then started. In analysis V15Hz, the same eccentric moment was assumed as in V23Hz $F_{dyn}/F_o = 2$, which reduced the applied dynamic force by a ratio of $15^2/23^2$ through the dependency on the frequency. In analysis V23Hz hook load, the applied static force was linearly increased from 20% to 100% of the self-weight over the initial 50 s of vibro-driving, modelling a hook load reduction from 80% to zero of the pile self-weight.

3 RESULTS AND DISCUSSION

3.1 Vibro-driven pile installation: overview

Pile tip penetration under self-weight (the initial 3 s of simulation time) is the same in the four analyses, $z = 0.48D$ (Fig. 2). The progression of pile penetration differs significantly during the vibro-driving phase:

- There was the expected significantly faster penetration in V23Hz $F_{dyn}/F_0 = 4$ compared to V23Hz $F_{dyn}/F_0 = 2$ due to the doubling of the dynamic load amplitude.
- V15Hz was expected to have resulted in the slowest penetration as $F_{dyn}/F_0 = 1.7$ (particularly in combination with the lower number of applied cycles per second) but faster penetration was observed than in V23Hz $F_{dyn}/F_0 = 2$.
- Retaining a percentage of the static force through hook load, i.e. lowering the static driving force as done in V23Hz hook load, resulted in an unexpectedly faster pile penetration compared to the analysis with the same set of conditions without hook load (V23Hz $F_{dyn}/F_0 = 2$).

The changes in soil state underpinning this response are investigated in the following.

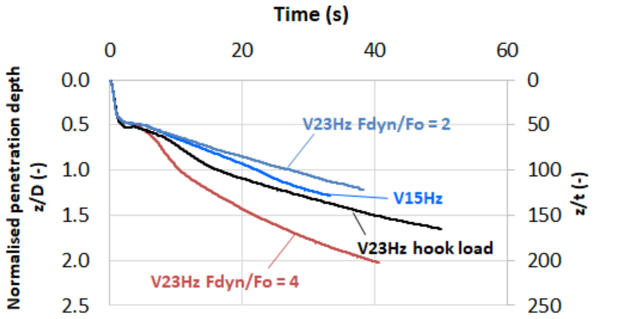

Figure 2. Pile penetration against simulation time (results shown for 24 h computational time for V23Hz hook load, all other analyses became numerically unstable)

3.2 Vibro-driven pile installation at 23 Hz: the effect of different F_{dyn}/F_0 ratios

The dynamic force, applied at a frequency of 23 Hz in V23Hz $F_{dyn}/F_0 = 2$, is consistent with an eccentric moment M_e = 359 kg.m. Considering the dynamic mass m_{dyn} = 1,500 t, the cyclic displacement amplitude without soil resistance is calculated as s_0 = 0.96 mm or $0.01t$. This is not expected to be sufficient to generate full reversal, especially to degrade the tip resistance. The low magnitude oscillations around the overall pile penetration trend is shown in detail in Figure 3.

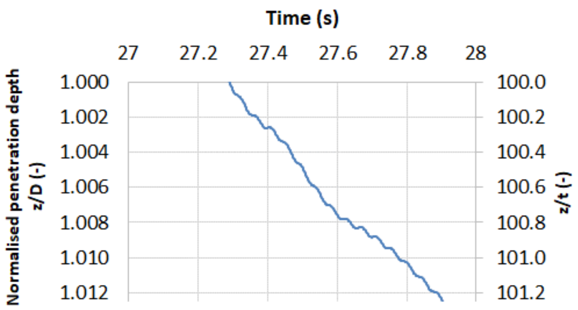

Figure 3. Enlarged view of pile penetration with time, vibro-driving at 23 Hz with a force ratio $F_{dyn}/F_0 = 2$

Indeed, the results show significant vertical effective stresses below the pile tip, but also substantial horizontal effective stresses outside the lower part of the pile shaft and importantly at pile tip level inside the pile (Figure 4a, b, shown after 30 s of vibro-driving when the pile has penetrated to 1.12D). Furthermore, positive excess pore pressures mean that the effective stresses are very low both inside the pile above tip level as well as outside the pile. In contrast, the zone of enhanced effective stresses is linked with dilation-induced negative excess pore pressures, which increases penetration resistance.

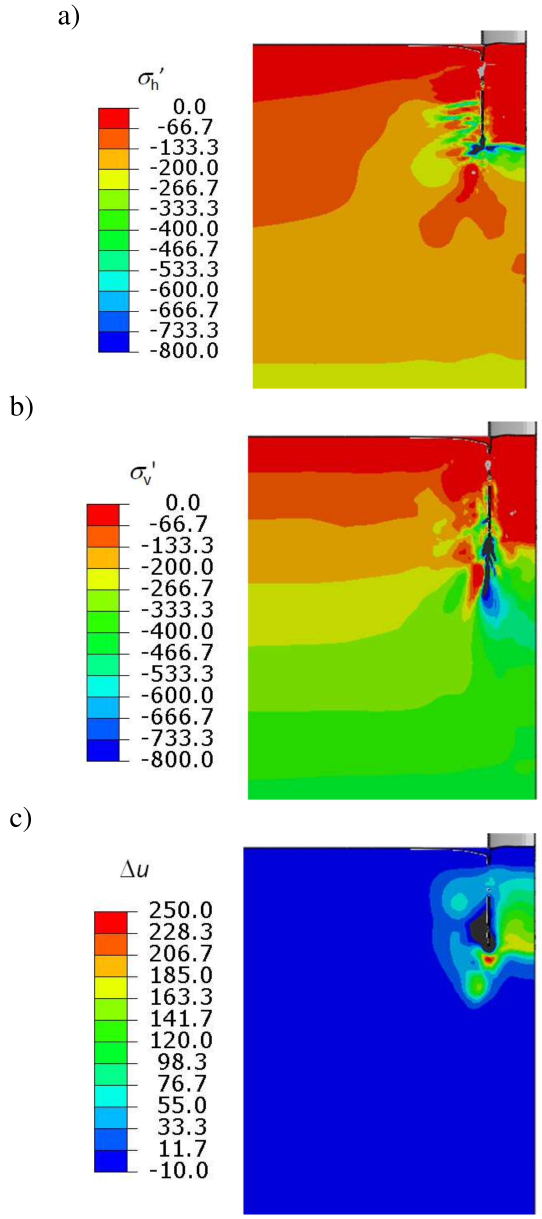

Figure 4. a) Horizontal and b) vertical effective stresses, c) excess pore pressures after 30 s of vibro-driving at 23 Hz with $F_{dyn}/F_0 = 2$ when $z/D = 1.12$

With larger dynamic forces (V23Hz $F_{dyn}/F_0 = 4$), the cyclic amplitude doubles according to Equation 3, though there is still insufficient movement to cause reversal and degrade tip resistance significantly through this mechanism. However, the increase of downward driving force ($F_0 + F_{dyn}$) in itself increases the pile penetration rate as shown in Figure 5. This increased shearing also significantly enhanced the magnitudes of the excess pore pressures, which shows large positive values inside and around most of the pile, importantly including around and below the pile tip as shown in Figure 6. Given that these pore pressures are mostly beneficial (i.e. reducing soil resistance to vibro-driving) this further facilitated pile penetration.

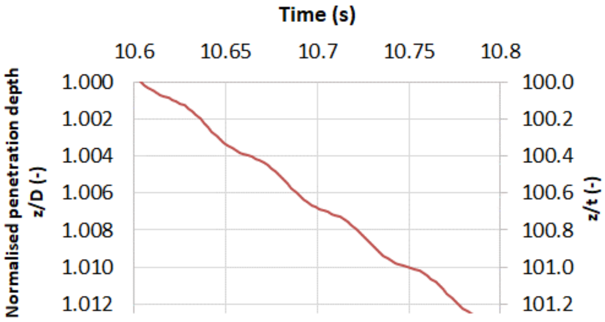

Figure 5. Enlarged view of pile penetration with time, vibro-driving at 23 Hz with a force ratio $F_{dyn}/F_0 = 4$

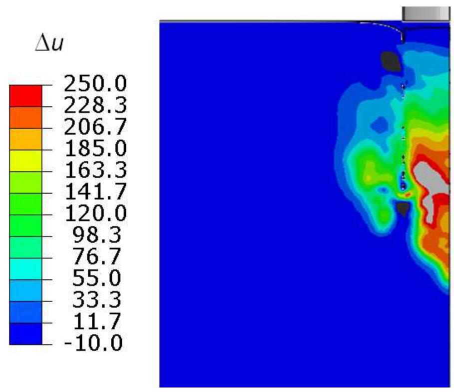

Figure 6. Excess pore pressures after 30 s of vibro-driving at 23 Hz with a force ratio $F_{dyn}/F_0 = 4$ when $z/D = 1.8$

The different dynamic load applied in V23Hz $F_{dyn}/F_0 = 2$ and V23Hz $F_{dyn}/F_0 = 4$ also resulted in starkly different acceleration fields, with the lower force ratio signifcantly accelerating a large mass of soil around the pile tip, while inertial effects were much more localised close to the pile wall and the tip for the higher force ratio.

3.3 Vibro-driven pile installation at 15 Hz

Accelerations are also localised to the lower pile shaft but radiate out further below the pile tip when the pile is vibrated at 15 Hz. The effective stresses and excess pore pressure fields (Figure 7) are overall similar to those in the 23 Hz analysis, though the horizontal effective stresses in Figure 7a show less arching inside the pile at the tip level. The positive excess pore pressures are higher and extend further below the pile tip inside the pile, which overall results in faster pile penetration despite the lower applied forces.

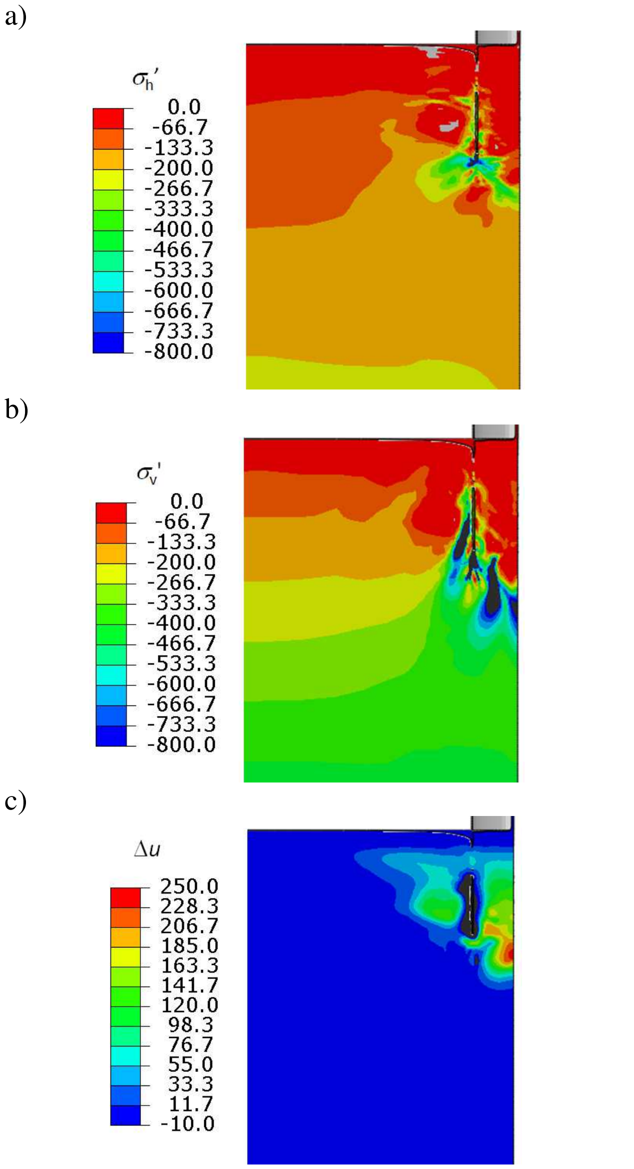

Figure 7. a) Horizontal and b) vertical effective stresses, c) excess pore pressures after 30 s of vibro-driving at 15 Hz

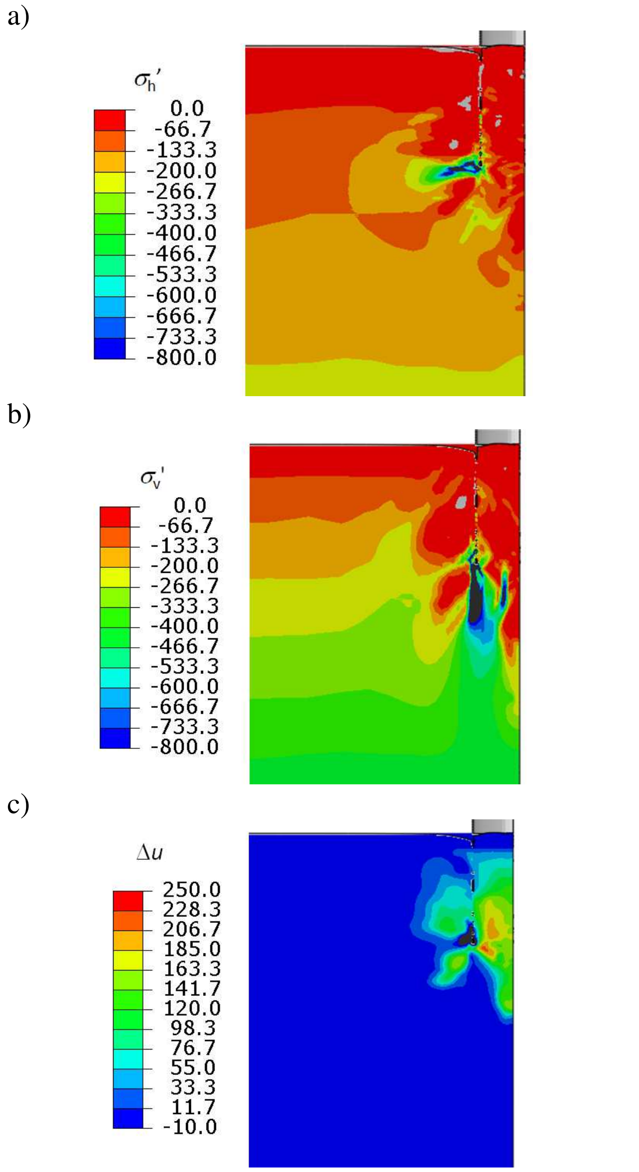

Figure 8. a) Horizontal and b) vertical effective stresses, c) excess pore pressures after 30 s of vibro-driving at 23 Hz with varying hook load when z/D = 1.4

3.4 Vibro-driven pile installation at 23 Hz with a varying hook load

Figure 8 shows the effective stresses and excess pore pressures after 30 s of vibro-driving which explain the unexpectedly faster installation than without hook load (Fig. 2). Holding back static driving force through the application of hook load, at least for the conditions assumed here, is beneficial as it leads to significant positive excess pore pressures in particular inside the pile and under the pile tip (Figure 8c). Horizontal effective stresses are very low: only outside the pile at the pile tip is there a relatively small area showing enlarged horizontal effective stresses (Figure 8a). Vertical effective stresses are also very low other than underneath the pile tip. Looking at the results in more detail (Fig. 9), it appears as though the response is periodic, with several cycles without significant further pile penetration followed by rapid penetration before penetration slows again.

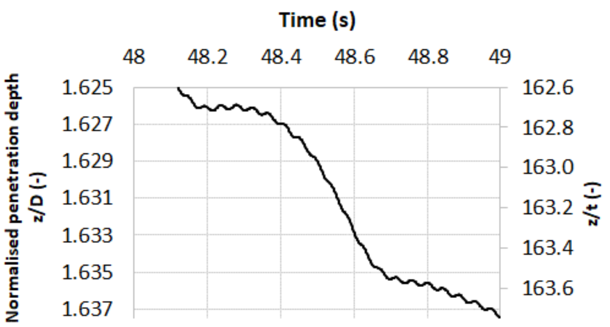

Figure 9. Enlarged view of pile penetration with time, vibro-driving at 23 Hz with varying hook load

In all analyses discussed here, changes in void ratio were observed, with densification (caused by cyclic loading) resulting in reduced effective stress as seen in the contour plots.

4 CONCLUSIONS

Numerical modelling has been used to gain insights into mechanisms underpinning vibro-driving of a large diameter monopile in dense saturated sand. Friction fatigue at the pile shaft, softening of the tip resistance through uplift, dynamic effects and excess pore pressures are all shown to be important, and the inter-relation between parameters that can be controlled during vibro-driving and the resulting response is complex. Somewhat counter-intuitively, lower driving force can have benefits in easing the penetration resistance, with the numerical results revealing the underlying changes in the state of the saturated sand.

AUTHOR CONTRIBUTION STATEMENT

Britta Bienen: Conceptualization, Numerical modelling, results analysis, Writing- Original draft. **Pourya Kazemi Esfeh, Fraser Bransby**: Writing-Reviewing and Editing. **Patrick Staubach**: Software (hydro-mechanical coupled user routine), Writing-Reviewing and Editing.

ACKNOWLEDGEMENTS

The authors are grateful for the financial support provided by the Australian Research Council Discovery Project DP200103466 "Understanding vibratory pile installation in sand and its effects on in-service pile response under lateral loading". The 3rd author is supported through the Fugro Chair in Geotechnics.

REFERENCES

Bienen, B., Fan, S., Schröder, M., Randolph, M.F. (2021). Effect of the installation process on monopile lateral response. *Geotechnical Engineering*, Vol. 174, No. 5, pp. 530-548.

Dierssen, G. (1994). *Ein bodenmechanisches Modell zur Beschreibung des Vibrationsrammens in körningen Böden*. PhD Thesis, University of Karlsruhe, Germany.

Fan, S., Bienen, B., Randolph, M.F. (2021). Effects of monopile installation on subsequent lateral response in sand, Part I: Pile installation. *Journal of Geotechnical and Geoenvironmental Engineering (ASCE)*, https://doi.org/10.1061/(ASCE)GT.1943-5606.0002467.

Hamann, T., Qiu, G., and Grabe, J. (2015). Application of a coupled Eulerian–Lagrangian approach on pile installation problems under partially drained conditions. *Comp. and Geotechnics*, 63, 279–290.

Kazemi Esfeh, P., Bienen, B., Bransby, M.F. (2025). Insights into pile vibro-driving in sand through numerical modelling. Submitted.

Massarsch, K.R., Wersäll, C., Fellenius, B.H. (2021). Vibratory driving of piles and sheet piles – state of practice. *Proc. Inst. Civil Engineers – Geotech. Eng.*, https://doi.org/10.1680/jgeen.20.00127.

Moriyasu, S., Kobayashi, S., Matsumoto, T. (2018). Experimental study on friction fatigue of vibratory driven piles by in situ model tests. *Soils and Foundations*, 58 (2018) 853–865.

Niemunis, A., and Herle, I. (1997). Hypoplastic model for cohesionless soils with elastic strain range. *Mech. Coh.-fric. Materials*, 2(4), 279–299.

Pawsey Supercomputing Research Centre. (2023). Setonix Supercomputer. Perth, Western Australia. https://doi.org/10.48569/18sb-8s43.

Rodger, A.A. and Littlejohn, G.S. (1980). A study of vibratory driving in granular soils. *Géotechnique*, 30(3):269-293.

Staubach, P., Machaček, J., Moscoso, M. C., and Wichtmann, T. (2020). Impact of the installation on the long-term cyclic behaviour of piles in sand: a numerical study. *Soil Dyn. and Earthquake Eng.*, https://doi.org/10.1016/j.soildyn.2020.106223.

Staubach, P., Machaček, J., Bienen, B. and Wichtmann, T. (2022). Long-term response of piles to cyclic lateral loading following vibratory and impact driving in water-saturated sand, *Journal of Geotechnical and Geoenvironmental Engineering (ASCE)*, https://doi.org/10.1061/(ASCE)GT.1943-5606.0002906.

Stein, P. (2023) *Stress state developments during the installation of pipe piles in sand and their influence on the lateral load-bearing behaviour.* Dissertation, Tech. Uni. Braunschweig, Germany.

Vogelsang, J. (2017). *Untersuchungen zu den Mechanismen der Pfahlrammung*. PhD Thesis, University of Karlsruhe, Germany.

von Wolffersdorff, P. (1996). A hypoplastic relation for granular materials with a predefined limit state surface. *Mech. Coh.-fric. Materials*, 1(3), 251–271.

Wichtmann, T. and Triantafyllidis, T. (2016a) An experimental data base for the development, calibration and verification of constitutive models for sand with focus to cyclic loading. Part I: tests with monotonic loading and stress cycles. *Acta Geotechnica*, 11(4): 739–761, https://doi.org/10.1007/s11440-0150402-z.